On the Development of Nonoverlapping and Stable Hybrid FETD-FDTD Formulations

Ali Akbarzadeh-Sharbaf, *Associate Member, IEEE*, and Dennis D. Giannacopoulos, *Senior Member, IEEE*

***Abstract*—A general framework to combine the finite-difference time-domain (FDTD) and the finite-element time-domain (FETD) formulations, both based on the vector wave equation, is proposed. In contrast to the existing stable hybrid FETD-FDTD, there is no transition layer between two subdomains. In addition, the stability of the proposed approach is analytically proved. This framework allows combining different FDTD and FETD formulations together. Particularly, a fully unconditionally stable hybrid method is proposed, which is proved to be energy conservative too. The key ingredient is a finite-element tearing and interconnecting method for electromagnetic problems with a new interface condition that preserves the stability of the numerical method in each region. Several numerical examples are considered in order to validate the proposed methods. The numerical results match with the reference solutions very well in all cases.**

***Index Terms*—Finite-difference time-domain (FDTD) method, finite-element tearing and interconnecting (FETI), finite-element time-domain (FETD) method, nonoverlapping.**

I. Introduction

THE finite-difference time-domain (FDTD) method and the finite-element time-domain (FETD) method are two powerful and versatile differential-based numerical techniques for the transient solution of electromagnetic problems [1]–[6]. However, each has their own pros and cons. The primary weakness of the FDTD is the staircase approximation. The simplest approach to improve accuracy is to refine the entire mesh uniformly, which can greatly increase the computational cost. Since in many practical situations only certain parts of the problem have significantly more complexity than the rest, a more efficient approach is to utilize subgridding techniques to refine the mesh just around the desired regions [7]–[9]. This approach is not also without shortcomings, because the implementation is more involved and the stability of the total method is limited by the most refined region. On top of that, all of the FDTD-based remedies share the same drawback: a staircase approximation can not guarantee the convergence of the solution, regardless of the level of refinement [10]. On the other hand, the FETD based on the VWE can be formulated in an US way, if the Newmark-β method is utilized. The unstructured mesh can take into account very complex objects in an accurate manner. However, the main drawback is its higher computational complexity. In such situations, a hybrid FETD-FDTD formulation can be very helpful in which only the most complex parts of the problem are discretized using the FETD method and the rest with the FDTD. Early attempts to combine these methods suffer from instability problems [11]–[15]. In 2000, the first stable hybrid method was developed by Rylander [16]. However, the FDTD and FETD regions are overlapped and only the conditionally stable (CS) leap-frog FDTD is utilized in the structured part, which makes the total hybrid method CS. In the only attempt to develop a fully US hybrid, highly dissipative results were obtained [17].

Finite-element tearing and interconnecting (FETI) is a type of domain decomposition method (DDM), which first *tears* the computational domain into several nonoverlapping subdomains and then *interconnects* the subproblems together by solving an interface problem defined on the boundaries between subdomains. Although the FETI is widely-used in frequency-domain methods [18], only a few formulations have been developed for the time-domain Maxwell's equation [19], [20]. All of them enforce the continuity of the tangential electric field between subdomains and no proof is provided to investigate the effect of FETI on the stability of the underlying FETD formulations in each subdomain.

In this paper, we propose a general approach to combine different variations of the FDTD and the FETD formulations. FDTD and FETD formulations are constructed from the VWE based on the fact that the spatial discretization of the FETD on brick-shaped elements is identical to the FDTD when the trapezoidal rule is employed for evaluating mass and stiffness matrices [21]. The methods are hybridized using a new time-domain FETI (TD-FETI). In contrast to the existing TD-FETIs in electromagnetics [19], [20], the tangential continuity of the first time derivative of the electric field is enforced between two regions. It can be shown that this condition can lead to a stable formulation [22], [23]. The proposed approach is proved to be stable as long as the stability condition of each region is satisfied. Furthermore, it has two distinct advantages over the previously-developed hybrid formulations: 1) There is no need to consider a transition region between two methods; 2) It is demonstrated that a fully US and energy conservative hybrid method can be constructed, which is free from dissipation or growth. The validity and accuracy of the proposed approach is tested through several numerical examples.

It is worth mentioning that the proposed TD-FETI can be directly employed as a DDM to reduce the computational burden

Manuscript received February 24, 2014; revised September 12, 2014; accepted September 13, 2014. Date of publication September 19, 2014; date of current version November 25, 2014. This work was supported by the Natural Sciences and Engineering Research Council (NSERC) of Canada.

The authors are with the Department of Electrical and Computer Engineering, McGill University, Montreal, QC H3A 0E9 Canada (e-mail: ali.akbarzadehsharbaf@mail.mcgill.ca; dennis.giannacopoulos@mcgill.ca).

Color versions of one or more of the figures in this paper are available online at http://ieeexplore.ieee.org.

Digital Object Identifier 10.1109/TAP.2014.2359496

of the large-scale transient electromagnetic problems using the FETD method.

II. FETD Formulations

A. FETD Formulation Based on the VWE

Discretizing the VWE in space using the curl-conforming basis functions gives a linear system of differential equations as [6]

$$[\mathcal{S}]\{e\} + [\mathcal{M}]\frac{\partial^2\{e\}}{\partial t^2} = \{f\} \tag{1}$$

where $\{e\} = [e_1, e_2, \ldots, e_{N_{ed}}]^T$ and

$$\mathcal{M}_{ij} = \int_\Omega \varepsilon \boldsymbol{N}_i \cdot \boldsymbol{N}_j dV \tag{2}$$

$$\mathcal{S}_{ij} = \int_\Omega \mu^{-1} \nabla \times \boldsymbol{N}_i \cdot \nabla \times \boldsymbol{N}_j dV \tag{3}$$

$$f_i = -\int_\Omega \boldsymbol{N}_i \cdot \frac{\partial \boldsymbol{\mathcal{J}}_{imp}(t)}{\partial t} dV \tag{4}$$

in which $\boldsymbol{N}$ and $\boldsymbol{\mathcal{J}}_{imp}(t)$ represent the vector edge basis function and electric impressed current, respectively. The Newmark-β method is usually employed to directly discretize (1), which involves the following approximations [24]

$$\begin{aligned}\{e\}^{n+1} - \{e\}^n = {} & \Delta t \frac{\partial\{e\}}{\partial t}^n + \beta \Delta t^2 \frac{\partial^2\{e\}}{\partial t^2}^{n+1} \\ & + \Delta t^2 \left(\frac{1}{2} - \beta\right) \frac{\partial^2\{e\}}{\partial t^2}^n \qquad (5a) \\ & \frac{1}{\Delta t}\left(\frac{\partial\{e\}}{\partial t}^{n+1} - \frac{\partial\{e\}}{\partial t}^n\right) \\ = {} & \frac{1}{2}\left(\frac{\partial^2\{e\}}{\partial t^2}^{n+1} + \frac{\partial^2\{e\}}{\partial t^2}^n\right) \qquad (5b)\end{aligned}$$

in which $0 \le 2\beta \le 1$. $(\partial\{e\}/\partial t)^n$ and $(\partial^2\{e\}/\partial t^2)^n$ denote the value of the first and second time derivatives of $\{e\}$ at $t = n\Delta t$. It is easy to extract the following relations from (5):

$$\begin{aligned}&\beta \frac{\partial\{e\}}{\partial t}^{n+1} + (1-2\beta)\frac{\partial\{e\}}{\partial t}^n + \beta \frac{\partial\{e\}}{\partial t}^{n-1} \\ &= \frac{\{e\}^{n+1} - \{e\}^{n-1}}{2\Delta t} \qquad (6a) \\ &\beta \frac{\partial^2\{e\}}{\partial t^2}^{n+1} + (1-2\beta)\frac{\partial^2\{e\}}{\partial t^2}^n + \beta \frac{\partial^2\{e\}}{\partial t^2}^{n-1} \\ &= \frac{\{e\}^{n+1} - 2\{e\}^n + \{e\}^{n-1}}{\Delta t^2}. \qquad (6b)\end{aligned}$$

The value of $\beta = 1/4$ results in an US formulation while $\beta = 0$ yields a CS formulation, which are equivalent to discretizing (1) using the trapezoidal rule and the central difference method, respectively, as can be validated by (6). For the sake of brevity, we call the VWE-based FETD method NB-FETD.

B. Mixed FETD and Equivalence to the FDTD

In contrast to the previous section, one can discretize the two first-order Maxwell's equations as follows [5]:

$$[\mathcal{M}]\frac{\partial\{e\}}{\partial t} = [\mathcal{C}]^T[\mathcal{M}_f]\{b\} \tag{7a}$$

$$\frac{\partial\{b\}}{\partial t} = -[\mathcal{C}]\{e\} \tag{7b}$$

where $[\mathcal{M}]$ is defined in (2) with $\boldsymbol{N}$ is replaced with the Whitney 1-form elements, $\boldsymbol{W}^{(1)}$, $[\mathcal{C}]$ is the discrete curl operator solely composed of $\pm$ 1 nonzero entries and

$$\mathcal{M}_{f_{ij}} = \int_\Omega \mu^{-1} \boldsymbol{W}_i^{(2)} \cdot \boldsymbol{W}_j^{(2)} dV \tag{8}$$

where $\boldsymbol{W}^{(2)}$ represents the Whitney 2-form elements. It can be shown that $[\mathcal{C}]^T[\mathcal{M}_f][\mathcal{C}]$ is identical to the stiffness matrix (3) for the Whitney elements [25]; hence, (7) becomes equivalent to (1).

The mixed FETD formulation (7) has a similar form to the FDTD method; hence, it can be considered as a generalization of the FDTD method to unstructured grids. In fact the standard FDTD method, before temporal discretization, can be written in the same matrix from as (7) in which $[\mathcal{M}]$ and $[\mathcal{M}_f]$ are replaced with $[\mathcal{M}^\dagger]$ and $[\mathcal{M}_f^\dagger]$, respectively. The matrices marked with "†" can be obtained from the original definitions by evaluating the integrals using the trapezoidal approximation instead of exact integration over the brick elements (mass-lumping) [21]. It should be noted that $[\mathcal{M}_f^\dagger]$, and consequently $[\mathcal{S}^\dagger]$, are identical to $[\mathcal{M}_f]$, and $[\mathcal{S}]$, in the 2-D case; however, it does not hold in 3-D [26]. These equivalences were also utilized in the development of stable FDTD subgridding techniques [7], [8].

The leap-frog method is the most widely-used approach to discretize (7) in time, which can be shown to be equivalent to the NB-FETD with $\beta = 0$. Recently, it has been shown that the same equivalence holds between the mixed FETD formulation discretized with the trapezoidal rule [known as the Crank-Nicolson (CN)-FETD [27]] and the NB-FETD with $\beta = 1/4$ [28].

From the discussion above it can be concluded that the NB-FETD with mass-lumped matrices and discretized with $\beta = 0$ and $\beta = 1/4$ is equivalent to the standard leap-frog FDTD and the CN-FDTD, proved to be US [4], respectively. The first equivalence has been utilized to develop the stable hybrid FETD-FDTD method with overlapping grids [16].

III. Time-Domain Finite-Element Tearing and Interconnecting

The finite-element formulation based on the variation principle involves finding a functional whose stationary point corresponds to the original governing differential equation. For the spatially-discretized VWE (1) such a functional can be found as [29]

$$\mathrm{F} = \frac{1}{2}\left(\frac{\partial\{e\}}{\partial t}\right)^T [\mathcal{M}]\frac{\partial\{e\}}{\partial t} - \frac{1}{2}(\{e\})^T[\mathcal{S}]\{e\} \tag{9}$$

in which the source term is omitted for simplicity.

However, in the conventional FETI formulation, the entire computational domain is divided into several, here one FE and one FD, nonoverlapping subdomains. In order to preserve the continuity of the solution, a condition must be enforced between subdomains. The conventional condition is the tangential continuity of the electric field [19]; however, we impose the continuity of the first time derivative of the electric field $((\partial\{e\}/\partial t))$ [22]. This constraint can be expressed as

$$[B_{FE}]^T \frac{\partial\{e_{FE}\}}{\partial t} + [B_{FD}]^T \frac{\partial\{e_{FD}\}}{\partial t} = \{0\} \tag{10}$$

where $[B_i]$ is a Boolean matrix to extract the degrees of freedom (DOFs) residing on the interface between two regions and $\{0\}$ is a zero vector of appropriate size. The $[B_{FE}]$ and $[B_{FD}]$ matrices are solely composed of $+1$ and -1 nonzero entries, or vice versa, respectively to enforce the continuity of $(\partial\{e\}/\partial t)$ on every DOF on the interface. The problem now involves finding the stationary point of the functional F in every subdomain by which the constraint (10) is also satisfied. The method of Lagrange multipliers is widely used to solve this constrained problem. We first need to augment the original functionals with the constraint by defining a new variable λ known as the Lagrange multiplier, as

$$\{\Lambda\} = \mathrm{F}_{FE} + \mathrm{F}_{FD} + \{\lambda\}\left([B_{FE}]^T \frac{\partial\{e_{FE}\}}{\partial t} + [B_{FD}]^T \frac{\partial\{e_{FD}\}}{\partial t}\right) \tag{11}$$

taking the first variation of the Lagrangian $\{\Lambda\}$ and integrating both sides shows that the solution of the original problem is equivalent to solving the following modified equation in each subdomain i

$$[\mathcal{S}_i]\{e_i\} + [\mathcal{M}_i]\frac{\partial^2\{e_i\}}{\partial t^2} = \{f_i\} - [B_i]\{\lambda\}. \tag{12}$$

Solving (12) for each subdomain together with the continuity condition (10) and discretizing them using the Newmark-β method, gives

$$\begin{aligned}[\mathcal{Q}_i]\frac{\partial^2\{e_i\}}{\partial t^2}^n &= -[\mathcal{S}_i]\{e\}^{n-1} - \Delta t[\mathcal{S}_i]\frac{\partial\{e_i\}}{\partial t}^{n-1} \\ &\quad - \Delta t^2(0.5-\beta_i)[\mathcal{S}_i]\frac{\partial^2\{e_i\}}{\partial t^2}^{n-1} \\ &\quad + \{f_i\}^n - [B_i]\{\lambda\}^n\end{aligned} \tag{13}$$

where $[\mathcal{Q}_i] = [\mathcal{M}_i] + \beta_i\Delta t^2[\mathcal{S}_i]$ and

$$\begin{aligned}&\left([B_{FD}]^T[\mathcal{Q}_{FD}]^{-1}[B_{FD}] + [B_{FE}]^T[\mathcal{Q}_{FE}]^{-1}[B_{FE}]\right)\{\lambda\}^n \\ &= \sum_{i=FD,FE}\Bigg\{[B_i]^T[\mathcal{Q}_i]^{-1}\{f_i\}^{n-1} - [B_i]^T[\mathcal{Q}_i]^{-1}[\mathcal{S}_i]\{e_i\}^{n-1} \\ &\quad + \left(\frac{2}{\Delta t}[B_i]^T - \Delta t[B_i]^T[\mathcal{Q}_i]^{-1}[\mathcal{S}_i]\right)\frac{\partial\{e_i\}}{\partial t}^{n-1} \\ &\quad + \left([B_i]^T + \Delta t^2(\beta_i - 0.5)[B_i]^T[\mathcal{Q}_i]^{-1}[\mathcal{S}_i]\right) \\ &\quad \times \frac{\partial^2\{e_i\}}{\partial t^2}^{n-1}\Bigg\}.\end{aligned} \tag{14}$$

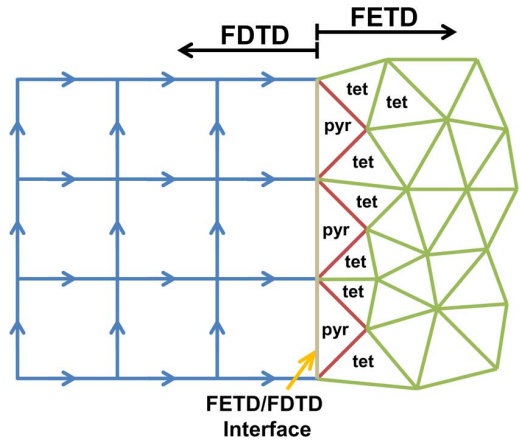

Fig. 1. Pyramidal elements are employed to connect the FETD unstructured mesh to the FDTD part.

Having obtained $(\partial^2\{e_i\}/\partial t^2)^n$, $\{e\}^n$ and $(\partial\{e_i\}/\partial t)^n$ can be evaluated using (5). In the case of the hybrid FETD-FDTD formulation, the matrices with $i = FD$ should be replaced with the †-signed ones to make the formulation spatially equivalent to the FDTD method in the structured region. As shown in Fig. 1, the pyramidal elements are employed to connect tetrahedra to brick elements in this case. It is instructive to note that if the formulation equivalent to the standard FDTD, mass-lumped matrices and $\beta_i = 0$, are utilized in both regions, $\{\lambda\}^n$ can be readily evaluated, because $[\mathcal{M}_i^\dagger]$ on brick-shaped elements is fully diagonal. This can be assumed as a domain decomposition method for the FDTD method. Furthermore, the procedure described above can be considered as a FETI method for just FETD with unstructured meshes in both, or multiple, regions.

At first glance, it seems from (14) that the explicit inverse of $[\mathcal{Q}_i]$'s are required to evaluate $\{\lambda\}^n$. This is a very memory-demanding task even for medium-size problems, particularly for unstructured parts, which would make the proposed methods hardly useful in practice. However, a closer look at (14) reveals that $[B_i]^T[\mathcal{Q}_i]^{-1}$ matrices are actually required for the update process. According to the nature of the Boolean matrix $[B_i]$, $[B_i]^T[\mathcal{Q}_i]^{-1}$ is equivalent to calculating a few rows of $[\mathcal{Q}_i]^{-1}$ corresponding to the interface DOFs. Each row of $[\mathcal{Q}_i]^{-1}$ can be evaluated by solving a linear system of equations. Since the $[\mathcal{Q}_i]$ matrix is already factorized for updating (13), the required rows of the inverse matrix can be obtained in a simple and efficient manner. This process has to be performed once, because the matrices are time-independent.

IV. Stability Analysis

In this section, we prove the stability of the proposed formulation. The stability analysis is carried out based on the energy method. This method is widely-used in mechanical and civil engineering [30]; however, it has found popularity in electromagnetic community in recent years [31]–[33]. The idea is to demonstrate that the energy of the method remains bounded during time stepping. For the sake of simplicity, we should first define the *jump* and *average* operators as follows:

$$[\![x^n]\!] = x^{n+1} - x^n \tag{15a}$$

$$\langle\langle x^n\rangle\rangle = x^{n+1} + x^n \tag{15b}$$

using the above operators, the following relations can be obtained from (5)

$$\left\langle\!\!\left\langle \frac{\partial\{e\}^n}{\partial t} \right\rangle\!\!\right\rangle = \frac{2}{\Delta t}[\![\{e\}^n]\!] + \Delta t(0.5-2\beta)\left[\!\!\left[\frac{\partial^2\{e\}^n}{\partial t^2} \right]\!\!\right] \tag{16a}$$

$$\left\langle\!\!\left\langle \frac{\partial^2\{e\}^n}{\partial t^2} \right\rangle\!\!\right\rangle = \frac{2}{\Delta t}\left[\!\!\left[\frac{\partial\{e\}^n}{\partial t} \right]\!\!\right] \tag{16b}$$

it is also easy to show that for any symmetric matrix $[A]$, we have

$$\langle\!\langle x^n \rangle\!\rangle^T [A] [\![x^n]\!] = [\![x^n]\!]^T [A] \langle\!\langle x^n \rangle\!\rangle = [\![(x^n)^T [A] x^n]\!]. \tag{17}$$

Consider the VWE FETD in each subdomain (12) as

$$[\mathcal{S}_i]\langle\!\langle \{e_i\}^n \rangle\!\rangle + [\mathcal{M}_i]\left\langle\!\!\left\langle \frac{\partial^2\{e_i\}^n}{\partial t^2} \right\rangle\!\!\right\rangle = -[B_i]\langle\!\langle \{\lambda\}^n \rangle\!\rangle \tag{18}$$

where the source term has been removed, because it has no effect on the stability. Multiplying both of (18) by $\langle\!\langle (\partial\{e_i\}/\partial t)^n \rangle\!\rangle^T$ and making use of (16), yields

$$\begin{aligned}&[\![\mathcal{E}^n_{e_i}]\!] + [\![\mathcal{E}^n_{m_i}]\!] \\ &\quad + 0.25\Delta t^2(0.5-2\beta_i)\left[\!\!\left[\frac{\partial^2\{e_i\}^n}{\partial t^2} \right]\!\!\right]^T [\mathcal{S}_i]\langle\!\langle \{e_i\}^n \rangle\!\rangle \\ &= -0.25\Delta t\left\langle\!\!\left\langle \frac{\partial\{e_i\}^n}{\partial t} \right\rangle\!\!\right\rangle^T [B_i]\langle\!\langle \{\lambda\}^n \rangle\!\rangle \end{aligned} \tag{19}$$

where

$$\mathcal{E}^n_{e_i} = \frac{1}{2}\left(\frac{\partial\{e_i\}^n}{\partial t}\right)^T [\mathcal{M}_i]\frac{\partial\{e_i\}^n}{\partial t} \tag{20a}$$

$$\mathcal{E}^n_{m_i} = \frac{1}{2}(\{e_i\}^n)^T [\mathcal{S}_i]\{e_i\}^n \tag{20b}$$

can be interpreted as the electric and magnetic energy in each subdomain at $t = n\Delta t$, respectively [33]. The summation of (19) over both subdomains results in the right-hand side vanishing due to the continuity condition (10). Using $\beta = 1/4$ in both regions, yields

$$\mathcal{E}^n_{e_t} + \mathcal{E}^n_{m_t} = \mathcal{E}^{n-1}_{e_t} + \mathcal{E}^{n-1}_{m_t} = \ldots = \mathcal{E}^1_{e_t} + \mathcal{E}^1_{m_t} \tag{21}$$

where subscript "t" denotes total contribution of all subdomains. This implies that the total electromagnetic energy of the proposed hybrid method is preserved during time stepping regardless of Δt, which not only shows the US stability of the method, but also demonstrates that the continuity condition (10) preserves the energy conservation property of the Newmark-β with $\beta = 1/4$.

The stability analysis becomes more involved for $\beta \neq 1/4$. Since the mass matrix is symmetric and positive-definite (SPD), we can multiply both sides of (12) by $[\mathcal{M}_i]^{-1}$ to obtain

$$\left[\!\!\left[\frac{\partial^2\{e_i\}^n}{\partial t^2} \right]\!\!\right] = -[\mathcal{M}_i]^{-1}[B_i][\![\{\lambda\}^n]\!] - [\mathcal{M}_i]^{-1}[\mathcal{S}_i][\![\{e_i\}^n]\!]. \tag{22}$$

Substituting (22) in (19) and making some simplifications, gives

$$\begin{aligned}&[\![\mathcal{E}^n_{e_i}]\!] + \left[\!\!\left[\tilde{\mathcal{E}}^n_{m_i}\right]\!\!\right] + [\![\mathcal{E}^n_{\lambda_i}]\!] \\ &= -0.25\Delta t\left\langle\!\!\left\langle \frac{\partial\{e_i\}^n}{\partial t} \right\rangle\!\!\right\rangle^T [B_i]\langle\!\langle \{\lambda\}^n \rangle\!\rangle \\ &\quad - \Delta t(0.25-\beta_i)\left[\!\!\left[\frac{\partial\{e_i\}^n}{\partial t} \right]\!\!\right]^T [B_i][\![\{\lambda\}^n]\!] \end{aligned} \tag{23}$$

where

$$\tilde{\mathcal{E}}^n_{m_i} = \frac{1}{2}(\{e_i\}^n)^T \underbrace{[\mathcal{S}_i]\left([\mathcal{I}] + \Delta t^2(\beta_i - 0.25)[\mathcal{M}_i]^{-1}[\mathcal{S}_i]\right)}_{[\tilde{\mathcal{S}}_i]}\{e_i\}^n \tag{24}$$

$$\mathcal{E}^n_{\lambda_i} = \Delta t^2(0.25-\beta_i)2(\{\lambda\}^n)^T [B_i]^T [\mathcal{M}_i]^{-1}[B_i]\{\lambda\}^n. \tag{25}$$

Note that (24) has an extra energy term compared to $\mathcal{E}^n_{m_i}$, which is generated by the time discretization method for $\beta \neq 1/4$ and exists in the conventional NB-FETD formulation too. The energy produced by the interface condition is given by (25). The summation of (23) over both subdomains causes the right-hand side to vanish due to the continuity condition (10). In order to have a nonincreasing energy, the $[\tilde{\mathcal{S}}_i]$ matrix in (24) has to be positive semi-definite (PSD). This condition is always satisfied for $\beta_i \geq 0.25$, which is the unconditional stability criterion of the original Newmark-β method. However, the PSD condition for $\beta_i < 0.25$ holds, if

$$\Delta t \leq \frac{(0.25-\beta_i)^{\frac{-1}{2}}}{\sqrt{\rho\left([\mathcal{M}_i]^{-1}[\mathcal{S}_i]\right)}} \tag{26}$$

where $\rho(\cdot)$ denotes the spectral radius of $(\cdot)$. The above condition is the same as the stability condition of the original NB-FETD. $\beta_i = 0$ simplifies it to

$$\Delta t \leq \frac{2}{\sqrt{\rho\left([\mathcal{M}_i]^{-1}[\mathcal{S}_i]\right)}}. \tag{27}$$

If one utilizes the †-signed matrices instead of conventional ones, it can be shown that (27) is equal to [34]

$$\Delta t \leq \Delta t_{CFL} = \frac{\sqrt{\mu\varepsilon}}{\sqrt{\frac{1}{(\Delta x)^2} + \frac{1}{(\Delta y)^2} + \frac{1}{(\Delta z)^2}}} \tag{28}$$

which is the stability condition of the leap-frog FDTD method. This is an expected result, because NB-FETD with $\beta = 0$ and mass-lumped matrices is equivalent to the FDTD method. Hence, they have to possess the same stability condition.

Now we turn our attention to the third term of the left-hand side (LHS) of (23), which is the contribution of the interface condition and was not present in the previous case with $\beta = 1/4$. In order to have a stable time stepping, this term must not be negative. Although we could not find such a bound on this term, the summation of (23) over both subdomains implies that

$$\mathcal{E}^n_{e_t} + \tilde{\mathcal{E}}^n_{m_t} + \mathcal{E}^n_{\lambda_t} = \mathcal{E}^{n-1}_{e_t} + \tilde{\mathcal{E}}^{n-1}_{m_t} + \mathcal{E}^{n-1}_{\lambda_t} = \ldots = \mathcal{E}^1_{e_t} + \tilde{\mathcal{E}}^1_{m_t} + \mathcal{E}^1_{\lambda_t}. \tag{29}$$

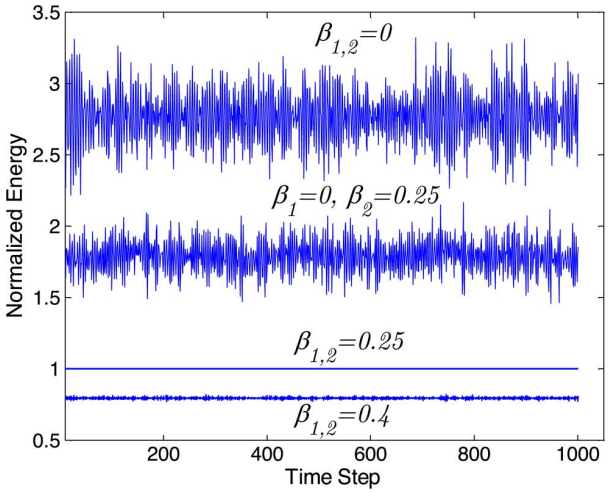

Fig. 2. Normalized energy $\mathcal{E}^n_{em_t}$ for all four scenarios during 1000 time steps.

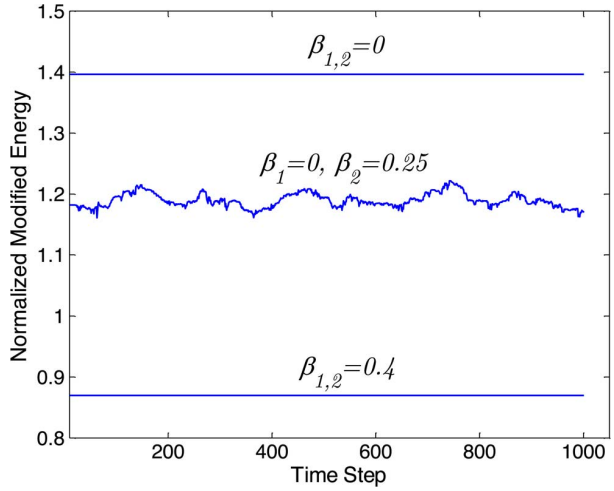

Fig. 3. Normalized modified energy $\tilde{\mathcal{E}}^n_{em\lambda_t}$ for three specified scenarios during 1000 time steps.

From the above equation we can conclude that $\mathcal{E}_{e_t} + \tilde{\mathcal{E}}_{m_t}$ remains bounded during time stepping, and hence, the method is stable, if $\mathcal{E}_{\lambda_t}$ remains bounded. By multiplying both sides of (14) by $\{\lambda\}^T$, it becomes evident that $\mathcal{E}_{\lambda_t}$ (25) is bounded as long as $\{e\}$ and its first and second time derivatives are bounded. Although this statement is perfectly valid for $\beta = 0$, we believe that this result can be extended to the other values of β, because $[\mathcal{M}]$ and $[\mathcal{Q}]$ share the same property: both are SPD. To summarize, we can subdivide the stability regions into three categories:

- $\beta_i = 1/4$: the method is US and preserves the energy conservation property of the original NB-FETD.
- $\beta_i < 1/4$: the method is CS with the stability condition (26). However, the total discrete energy differs from the original energy definition. There are two extra contributions in the discrete energy: one from the interface condition and the other from the asymmetry of (5a) for $\beta \neq 1/4$.
- $\beta_i > 1/4$: the method has the same energy properties as the previous case, but it is US.

In order to validate the stability analysis results, we conducted a simple numerical example: a 1-D cavity divided into two subdomains and glued to each other using the proposed method. The cavity is excited with a randomly distributed initial vector, identical for all cases. Four different scenarios are considered: both regions with the same $\beta_{1,2} = 0, 0.25$ and 0.4 and in the last scenario one subdomain with $\beta_1 = 0$ and the other with $\beta_2 = 0.25$. In the first, third and fourth cases, two energy norms are calculated: $\mathcal{E}^n_{em_t} = \sum_i (\mathcal{E}^n_{e_i} + \mathcal{E}^n_{m_i})$ and $\tilde{\mathcal{E}}^n_{em\lambda_t} = \sum_i (\mathcal{E}^n_{e_i} + \tilde{\mathcal{E}}^n_{m_i} + \mathcal{E}^n_{\lambda_i})$. However, in the second case, $\beta_{1,2} = 0.25$, only $\mathcal{E}^n_{em_t}$ is considered, because the interface condition has no contribution to the energy of the method. In all cases the results are normalized with respect to the $\mathcal{E}^n_{em_t}$ energy for $\beta_{1,2} = 0.25$ example. The time step is set to 95% of the stability condition (27).

Fig. 2 shows the values of $\mathcal{E}^n_{em_t}$ within 1000 time steps for all scenarios. As can be seen, the energy remains bounded during time stepping in all cases; however, $\beta_{1,2} = 0.25$ is the only case that exactly preserves energy of the problem. The modified energy $\tilde{\mathcal{E}}^n_{em\lambda_t}$ for each three mentioned scenarios is depicted in Fig. 3. The modified energy remains bounded in all three cases and is exactly preserved as long as both subdomains are discretized using the same β, as dictated by (29). The fluctuations in the energy with $\beta_1 \neq \beta_2$ has a logical explanation: the contributions of the interface condition and the extra term that appear in $[\tilde{\mathcal{S}}]$ of the modified energy do not match for subdomains with different β's, but it remains bounded.

V. Numerical Examples

In this section, we provide three numerical examples to validate the proposed hybrid formulations. Among different possibilities for hybrid FETD-FDTD, we choose two of them to be considered in this section. One of them is a fully US hybrid method in which $\beta = 1/4$ is utilized in both subdomains, which is called "US hybrid" (equivalent to hybrid CN-FDTD and NB-FETD with $\beta = 1/4$) and the other employs $\beta = 0$ and 0.25 in the structured and unstructured regions, respectively. The latter method is named "CS hybrid", which is equivalent to combining the leap-frog FDTD with NB-FETD with $\beta = 1/4$. In all examples the time step for the CS hybrid is 95% of the maximum allowable time step in the standard FDTD method (28) ($\Delta t_{CS} = 0.95 \Delta t_{CFL}$). The time step for the US hybrid is set to $\Delta t_{US} = 2\Delta t_{CS}$. The structured part is discretized using relatively large cubical elements and the unstructured part is meshed by the Salome open source mesh generator [35], which is capable of producing transition pyramidal elements to connect brick-shaped elements to the tetrahedral elements.

Table I shows the required time for computation of a single time step of the FDTD part using both hybrid methods for every problem. A similar direct solver is employed in both cases. As can be seen, the CS hybrid method is at least around 2 times faster than the US method and becomes faster as the number of interface DOFs are decreased. Exploiting the sparsity of the LHS matrix in the CS case would result in a further speedup. It should be noted that taking into account the FETD part, excitation, boundary conditions, and the other parts of a practical implementation makes the required time for a single complete time step almost the same. That is where the US hybrid method can solve a problem faster in a certain physical time window compared to the CS one because of the larger time step.

TABLE I
COMPARISON OF THE COMPUTATION TIMES BETWEEN US AND CS HYBRID METHODS IN DIFFERENT EXAMPLES

Problem	Hybrid Method	length $[\mathcal{Q}_{FD}]$	No. of Shared DOFs	FDTD Part Time-Marching Time (per step)
Cavity	US	17304	1728	47.5 msec
	CS			27.7 msec
Bow-Tie	US	27840	1023	71.7 msec
	CS			29.4 msec
CCLR	US	20540	552	51.2 msec
	CS			13.0 msec

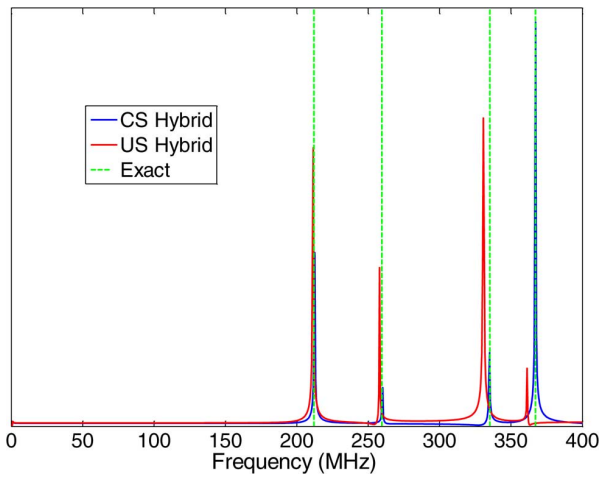

Fig. 4. Resonance frequencies of the cavity.

TABLE II
CALCULATED RESONANCE FREQUENCIES OF THE CAVITY. ALL VALUES ARE IN MHZ

	Mode #1	Mode #2	Mode #3	Mode #4
CS Method	212.62	260.17	335.06	367.31
Absolute Error	0.64	0.55	0.12	0.14
US Method	211.53	257.99	330.68	361.29
Absolute Error	0.46	1.64	4.49	5.88
Exact	211.99	259.63	335.18	367.17

A. Resonance Frequencies of a Cubic Cavity

The first example involves calculating the resonance frequencies of a $1\times1\times1$ m^3 cubical metallic cavity. A $0.6\times0.6\times0.6$ m^3 region located at the center of the cavity is discretized with tetrahedral elements. This region is wrapped by four layers of 5 cm wide cubical elements. The simulation consists of 10,000 time steps in the US case and 20,000 in the CS case, to make the simulation time the same.

Fig. 4 shows the first four excited modes obtained by either of methods along with the analytical solutions. No spurious mode is produced because of the interface condition. In order to study the accuracy more easily, we have calculated the error of each mode in Table II. As can be seen, all results match with the exact solutions very well. In addition, the error of the US hybrid method is generally more than the CS method, because of the larger time step, particularly for the higher modes, as expected.

B. Waveguide loaded with a Bow-tie-shaped Metallic Post

The second example is a waveguide filter with a bow-tie-shaped metallic post [36]. A bow-tie-shaped metallic post is placed inside a standard WR-90 waveguide with the cross-section of 22.86 mm $\times$ 10.16 mm. Fig. 5 shows the top view of the problem. The bow-tie-shaped post is composed of two concentric cylinders with the radii of $r_1 = 1.5$ mm and $r_2 = 5$ mm, respectively. The sectors of the larger cylinder have the angle of $\theta = 70°$. The metallic post is placed $d = 5.43$ mm away from the waveguide wall. The post is extended over the entire waveguide height along the z direction. As shown in Fig. 5, just a limited volume around the post is discretized with the unstructured mesh and the rest with 0.846 mm ($\simeq \lambda/30$, where λ is the wavelength of the highest frequency of interest, i.e., 13 GHz) cubical elements. The dominant TE_{10} mode is incident on Port 1 with a Blackman-Harris pulse shape.

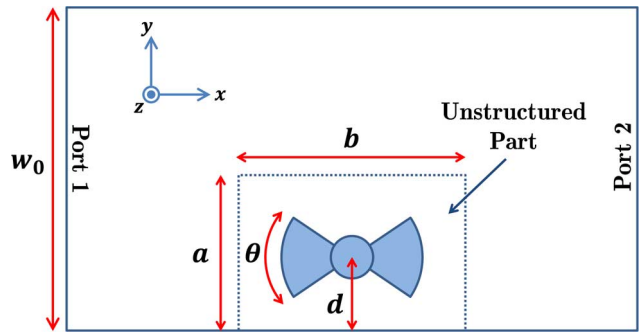

Fig. 5. Top view of the waveguide filter. The dimensions of the unstructured region are $a \simeq 11.00$ mm (13 cells) and $b \simeq 16.08$ mm (19 cells). $w_0 = 22.86$ mm is the width of the waveguide.

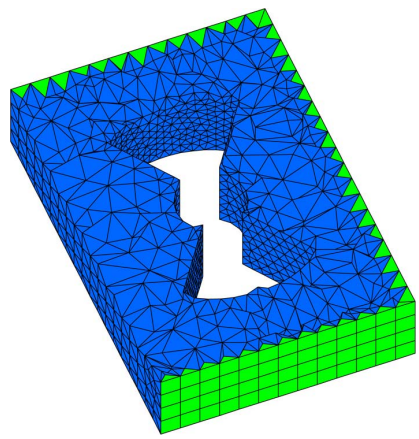

Fig. 6. Cut of the unstructured part of the mesh pertaining to the bow-tie-shaped filter. The pyramidal elements are colored in green.

The reflection coefficient is calculated using both US and CS hybrid methods and depicted in Fig. 7 along with the FDTD reference solution taken from [36]. There is a very good agreement between our results and the reference one.

C. Cross Circular Loop Resonator (CCLR)

The last example involves calculating the transmission coefficient of a dual-band Cross Circular Loop Resonator (CCLR) metamaterial [37]. Fig. 8 shows the structure composed of two CCLR unit cells in horizontal position. Simulating such a delicate structure using the FDTD requires an extremely refined grid and a very small time step. It is designed on a 0.5 mm thick

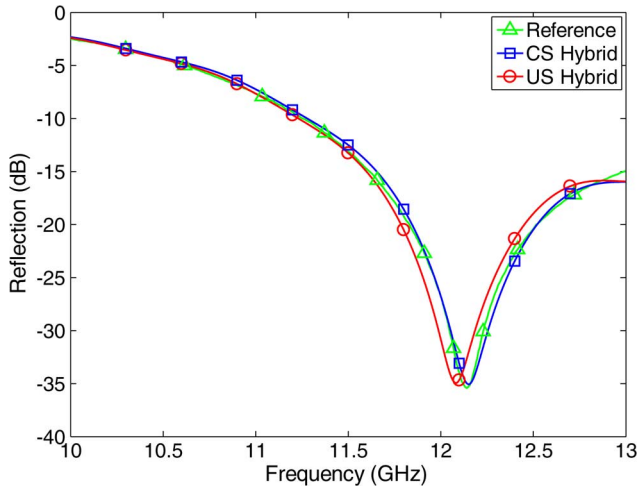

Fig. 7. Computed reflection coefficients using the proposed methods along with the FDTD reference solution [36].

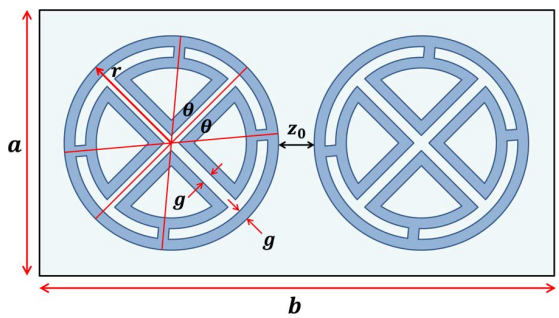

Fig. 8. Dual-band CCLR shown in the horizontal position. The dimensions are as follows: $r = 2.2$ mm, $a = 5$ mm, $b = 10.16$ mm, $z_0 = 0.6$ mm, $g = 0.1$ mm, and $\theta = 40^\circ$.

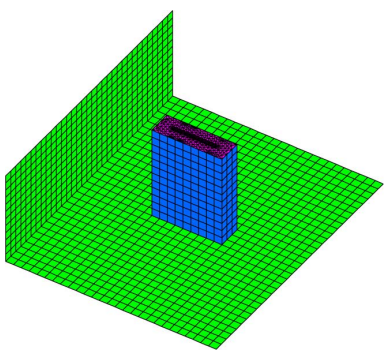

Fig. 9. Unstructured mesh around the CCLR metamaterial placed in the middle of the waveguide. Two sides of the waveguide are removed for the sake of clarity.

substrate with the relative permittivity of $\varepsilon_r = 3.55$. The tangent loss of the substrate is not included in the simulation. The metamaterial is placed in the middle of a WR-90 waveguide (see Fig. 9). The simulation details are the same as the bow-tie-shaped filter. The reference solution is obtained by solving the whole problem using NB-FETD with $\beta = 1/4$ and $\Delta t = \Delta t_{US}$ denoted as "Full FETD" (on the same mesh without TD-FETI).

The transmission coefficients obtained using three different methods are depicted in Fig. 10. All results match with each

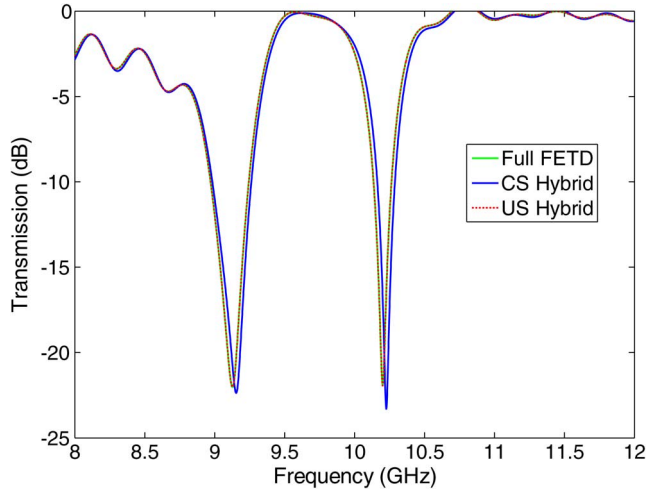

Fig. 10. Computed transmission coefficients using the proposed methods along with the full FETD result as the reference. In our opinion, fluctuations and resulting slightly positive values are due to utilizing a coarse grid in the FDTD part.

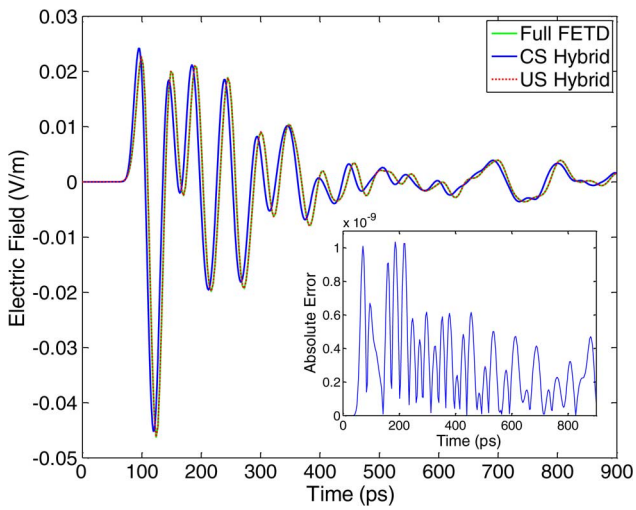

Fig. 11. Time-domain signals recorded on Port 2 using three different methods. The inset shows the absolute error between the reference (full FETD) and US hybrid samples.

other very well. Particularly, the US hybrid result is almost identical to the reference solution. Fig. 11 shows the time-domain electric field recorded on Port 2. The same similarity exists between time-domain signals. The absolute error between the US hybrid and the reference solution is plotted as inset, which shows a negligible error.

VI. Conclusion

In this paper, a novel and general approach to hybridize different formulations of the FETD and FDTD has been proposed. The idea is to utilize a new FETI algorithm to combine formulations in a nonoverlapping and stable manner. In addition, it has been shown that the hybrid method is stable as long as the stability condition of each subdomain is satisfied. The validity and accuracy of the proposed approach has been tested through several numerical examples.

REFERENCES

[1] A. Taflove and S. Hagness, *Computational Electrodynamics: The Finite-Difference Time-Domain Method*, 3rd ed. Boston, MA, USA: Artech House, 2005.

[2] K. S. Yee, "Numerical solution of initial boundary value problems involving Maxwell's equations in isotropic media," *IEEE Trans. Antennas Propag.*, vol. 14, no. 3, pp. 302–307, Mar. 1966.

[3] T. Namiki, "3-D ADI-FDTD method-unconditionally stable time-domain algorithm for solving full vector Maxwell's equations," *IEEE Trans. Microw. Theory Techn.*, vol. 48, no. 10, pp. 1743–1748, Oct. 2000.

[4] G. Sun and W. C. Trueman, "An unconditionally-stable FDTD method based on the Crank-Nicolson scheme for solving the three-dimensional Maxwell's equations," *Electron. Lett.*, vol. 40, no. 10, pp. 589–590, May 2004.

[5] M.-F. Wong, O. Picon, and V. Fouad Hanna, "A finite element method based on Whitney forms to solve Maxwell equations in the time domain," *IEEE Trans. Magn.*, vol. 31, no. 3, pp. 1618–1621, Mar. 1995.

[6] J. F. Lee and Z. Sacks, "Whitney elements time domain (WETD) methods," *IEEE Trans. Magn.*, vol. 31, no. 3, pp. 1325–1329, May 1995.

[7] N. V. Venkatarayalu *et al.*, "A stable FDTD subgridding method based on finite element formulation with hanging variables," *IEEE Trans. Antennas Propag.*, vol. 55, no. 3, pp. 907–915, Mar. 2007.

[8] R. A. Chilton and R. Lee, "Conservative and provably stable FDTD subgridding," *IEEE Trans. Antennas Propag.*, vol. 55, no. 9, pp. 2537–2549, Sep. 2007.

[9] M. Abalenkovs *et al.*, "Huygens subgridding for 3-D frequency-dependent finite-difference time-domain method," *IEEE Trans. Antennas Propag.*, vol. 60, no. 9, pp. 4336–4344, Sep. 2012.

[10] A. C. Cangellaris and D. B. Wright, "Analysis of the numerical error caused by the stair-stepped approximation of a conducting boundary in FDTD simulations of electromagnetic phenomena," *IEEE Trans. Antennas Propag.*, vol. 39, no. 10, pp. 1518–1525, Oct. 1991.

[11] D. J. Riley and C. D. Turner, "Interfacing unstructured tetrahedron grids to structured-grid FDTD," *IEEE Microw. Guided Wave Lett.*, vol. 5, no. 9, pp. 284–286, Sep. 1995.

[12] R. B. Wu and T. Itoh, "Hybrid finite-difference time-domain modeling of curved surfaces using tetrahedral edge elements," *IEEE Trans. Antennas Propag.*, vol. 45, no. 8, pp. 1302–1309, Aug. 1997.

[13] A. Monorchio and R. Mittra, "Time-domain (FE/FDTD) technique for solving complex electromagnetic problems," *IEEE Microw. Guided Wave Lett.*, vol. 8, no. 2, pp. 93–95, Feb. 1998.

[14] S. Selleri *et al.*, "Comparison between FDTD and hybrid FDTD-FETD applied to scattering and antenna problems," *Microw. Opt. Technol. Lett.*, vol. 18, no. 4, pp. 247–250, 1998.

[15] C. T. Hwang and R. B. Wu, "Treating late-time instability of hybrid finite-element/finite-difference time-domain method," *IEEE Trans. Antennas Propag.*, vol. 47, no. 2, pp. 227–232, Feb. 1999.

[16] T. Rylander and A. Bondeson, "Stable FEM-FDTD hybrid method for Maxwell's equations," *Comput. Phys. Commun.*, vol. 125, no. 1–3, pp. 75–82, 2000.

[17] A. A. Sharbaf and R. Sarraf-Shirazi, "An unconditionally stable hybrid FETD-FDTD formulation based on the alternating-direction implicit algorithm," *IEEE Antennas Wireless Propag. Lett.*, vol. 9, pp. 1174–1177, 2010.

[18] Y. Li and J.-M. Jin, "A new dual-primal domain decomposition approach for finite element simulation of 3-D large-scale electromagnetic problems," *IEEE Trans. Antennas Propag.*, vol. 55, no. 10, pp. 2803–2810, Oct. 2007.

[19] U. D. Navsariwala and S. D. Gedney, "An efficient implementation of the finite-element time-domain algorithm on parallel computers using a finite-element tearing and interconnecting algorithm," *Microw. Opt. Technol. Lett.*, vol. 16, no. 4, pp. 204–208, Nov. 1997.

[20] L. Du *et al.*, "An efficient time-domain method analysis of quasiperiodic structures by a finite-element tearing and interconnecting algorithm," *Microw. Opt. Technol. Lett.*, vol. 52, no. 5, pp. 1072–1078, May 2010.

[21] G. Cohen and P. Monk, "Gauss point mass lumping schemes for Maxwell's equations," *Numer. Methods Partial Differential Eq.*, vol. 14, no. 1, pp. 63–88, 1998.

[22] A. Gravouil and A. Combescure, "Multi-time-step explicit-implicit method for non-linear structural dynamics," *Int. J. Numer. Meth. Eng.*, vol. 50, no. 1, pp. 199–225, Jan. 2001.

[23] S. Karimi and K. B. Nakshatrala, "On multi-time-step monolithic coupling algorithms for elastodynamics," *J. Comput. Phys.*, vol. 273, pp. 671–705, 2014.

[24] N. Newmark, "A method of computation for structural dynamics," *J. Eng. Mech. Div.*, vol. 85, pp. 67–94, Jul. 1959.

[25] B. A. He and F. L. Teixeira, "Geometric finite element discretization of Maxwell equations in primal and dual spaces," *Phys. Lett. A*, vol. 349, pp. 1–14, 2006.

[26] R. Lee, "A note on mass lumping in the finite element time domain method," *IEEE Trans. Antennas Propag.*, vol. 54, no. 2, pp. 760–762, Feb. 2006.

[27] M. Movahhedi *et al.*, "Alternating-direction implicit formulation of the finite-element time-domain method," *IEEE Trans. Microw. Theory Techn.*, vol. 55, no. 6, pp. 1322–1331, Jun. 2007.

[28] A. Akbarzadeh-Sharbaf and D. D. Giannacopoulos, "Finite-element time-domain solution of the vector wave equation in doubly dispersive media using Möbius transformation technique," *IEEE Trans. Antennas Propag.*, vol. 61, no. 8, pp. 4158–4166, Aug. 2013.

[29] J.-M. Jin, *The Finite Element Method in Electromagnetics*, 2nd ed. Hoboken, NJ, USA: Wiley, 2003.

[30] T. J. R. Hughes, *The Finite Element Method: Linear Static and Dynamic Finite Element Analysis*. Upper Saddle River, NJ, USA: Prentice-Hall, 1987.

[31] F. Kung and H. T. Chuah, "Stability of classical finite-difference time-domain (FDTD) formulation with nonlinear elements-A new perspective," *Progr. Electromagn. Res.*, vol. 42, pp. 49–89, 2003.

[32] F. Edelvik, R. Schuhmann, and T. Weiland, "A general stability analysis of FIT/FDTD applied to lossy dielectrics and lumped elements," *Int. J. Numer. Model.*, vol. 17, pp. 407–419, 2004.

[33] F. Edelvik *et al.*, "An unconditionally sable subcell model for arbitrarily oriented thin wires in the FETD method," *IEEE Trans. Antennas Propag.*, vol. 51, no. 8, pp. 1797–1805, Aug. 2003.

[34] T. Rylander and A. Bondeson, "Stability of explicit-implicit hybrid time-stepping schemes for Maxwell's equations," *J. Comput. Phys.*, vol. 179, no. 2, pp. 426–438, 2002.

[35] SALOME, Project website [Online]. Available: http://www.salome-platform.org

[36] R. Lech and J. Mazur, "Tunable waveguide filter with bow-tie metallic posts," in *Proc. Inst. Elect. Eng., Microw., Antennas, Propag.*, Apr. 2004, vol. 151, no. 2, pp. 156–160.

[37] Z. Zhong *et al.*, "Dual-band negative permittivity metamaterial based on cross circular loop resonator with shorting stubs," *IEEE Antennas Wireless Propag. Lett.*, vol. 11, pp. 803–806, 2012.

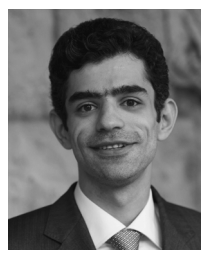

Ali Akbarzadeh-Sharbaf (A'14) received the M.Sc. degree in electrical engineering from Amirkabir University of Technology (Tehran Polytechnic), Tehran, Iran, in 2011. He is currently pursuing the Ph.D. degree at the Computational Analysis and Design Laboratory (CAD Lab), Department of Electrical and Computer Engineering, McGill University, Montréal, QC, Canada.

Mr. Akbarzadeh-Sharbaf is a recipient of the Iran Telecommunication Research Center (ITRC) grant to support his M.Sc. thesis. He is also a recipient of the McGill Engineering Doctoral Award (MEDA) and the Eric. L. Adler fellowship in electrical engineering, McGill University.

Dennis D. Giannacopoulos (SM'13) received the B.Eng. and Ph.D. degrees in electrical engineering from McGill University, Montreal, QC, Canada, in 1992 and 1999, respectively.

He has been with the Department of Electrical and Computer Engineering, McGill University, since 2000, where he is currently an Associate Professor and a member of the Computational Electromagnetics Group. His research interests include adaptive finite element analysis for electromagnetics and the acceleration of computational electromagnetics algorithms on emerging parallel architectures. He has authored or coauthored more than 90 referred journal and conference publications.

Dr. Giannacopoulos has twice been the recipient of his department's Professor of the Year Award. His students have received three best-paper/presentation awards at international conferences and symposia. His research has been sponsored by the Natural Sciences and Engineering Research Council of Canada (NSERC), the Fonds de recherche du Québec-Nature et technologies (FQRNT), and the Canada Foundation for Innovation (CFI). He has served on the editorial boards and technical program committees of several major international conferences and served as Co-Chair of the editorial board for the 14th Conference on the Computation of Electromagnetic Fields. He is a member of the International Compumag Society and the Ordre des Ingénieurs du Québec.